Analysis of Affinity and Specificity in an EF-Hand Site Using Double Mutant Cycles†

Tharin M. A. Blumenschein and Fernando C. Reinach*

Depto. de Bioquímica, Instituto de Química, Universidade de São Paulo, Av. Prof. Lineu Prestes, 748-São Paulo, SP-CEP 05508-900, Brazil

Received October 25, 1999; Revised Manuscript Received January 21, 2000

ABSTRACT: The effects of three mutations on the EF-hand Ca^{2+}/Mg^{2+} binding site of smooth muscle myosin regulatory light chain (RLC) were studied: D5S, in which an aspartate is replaced by a serine in position 5 of the loop; D9E, in which an aspartate is replaced by a glutamate in position 9; and D12E, in which the aspartate in position 12 is replaced by a glutamate. All possible combinations of the three mutations were produced. The single mutants D5S and D9E and the double mutant D5S/D9E have low affinity for Ca^{2+}. All the mutants containing mutation D12E are Ca^{2+}-specific and have higher affinities than wild type, even when containing mutations D5S or D9E. All of the mutants studied have lower affinity for Mg^{2+} than the wild-type protein. As expected, the changes in binding free energy that each mutant produces depend on the residues present at the other positions of the site, since the mutated positions are very close in the protein structure. Coupling energies are about the same for all pairs of mutants when binding Ca^{2+}, but can have different values when binding Mg^{2+}. D5S and D9E have a large negative coupling energy for Mg^{2+} binding which suggests an interaction between these two positions. When mutation D12E is present, the coupling energy for Mg^{2+} binding between D5S and D9E is much lower, suggesting that this interaction occurs only if an aspartate is in position 12. Glutamate in position 9 may be able to coordinate Mg^{2+} directly in the double mutant D5S/D9E.

In biological systems, Ca^{2+} ions have an important role as intracellular messengers (*1*), while Mg^{2+} ions have structural and catalytic functions and act as counterions (*2*). These different functions are possibe due to their selective binding by regulatory proteins (*3*), which must be able to sense changes in Ca^{2+} concentration from $\sim 10^{-7}$ to $\sim 10^{-5}$ M (*4*) in the presence of millimolar Mg^{2+} concentrations. The exact determinants of divalent cation affinity and specificity are not fully understood (*3*, *5*).

In many of these regulatory proteins, the ion binds to an EF-hand site (*3*). These sites can modulate regulatory proteins, buffer Ca^{2+} concentration, or maintain protein structure (*3*). Regulatory sites are Ca^{2+}-specific, while structural sites bind both Ca^{2+} and Mg^{2+} (*3*, *6*, *7*).

An EF-hand site is constituted of 2 α-helices connected by a 12 amino acid loop (*8*). Six amino acids from the loop (positions 1, 3, 5, 7, 9, and 12) are responsible for coordinating the ion, either directly or indirectly through a water bridge. Usually, two EF-hand sites are tightly associated in a domain (*3*). Many proteins in this family are constituted by two such domains connected by a helix, as in calmodulin and troponin C (*3*, *9*).

Site-directed mutagenesis studies in metal-coordinating positions have been carried out in many EF-hand proteins. Linse and Forsén (*7*) summarized the mutagenesis studies published up to 1995. At that point, it was clear that the removal of an ion ligand always lead to a great reduction in affinity, and the replacement of the glutamate in position 12 by a monodentate ligand also resulted in a great loss of affinity. Replacements of a negatively charged amino acid by a neutral one usually lowers the site affinity, but the exchange of aspartate by glutamate, or vice-versa, can have different results depending on the position, neighboring amino acids, and probably even the overall site conformation.

Chicken smooth muscle (gizzard) myosin regulatory light chain (RLC)[1] is a good model to study the properties of EF-hand sites because it has only one site that binds both Ca^{2+} and Mg^{2+} and retains its metal binding properties even when the RLC is dissociated from the other myosin chains (*10*).

RLC is 171 amino acids long (*11*) and is highly homologous to calmodulin. As calmodulin, RLC has four EF-hand sites, although three of these sites are inactive, because of deletions or positive charges in positions that should coordinate the ion (*12*). The protein is divided in two domains, linked by a helix. The N-terminal domain contains the active EF-hand site (I) and a residual site, while the C-terminal domain contains two residual sites. The only active site is the closest to the N-terminus, and its loop starts at Asp 41. In contrast to the cardiac troponin C where the inactivated site is site I, in RLC the only active site is site I.

†This work was supported by the Fundação de Amparo à Pesquisa do Estado de São Paulo, Conselho Nacional de Pesquisa (Brazil). F.C.R. is an international fellow from The Howard Hughes Medical Institute. T.M.A.B. is a graduate fellow from FAPESP. Portions of this work were presented at the Biophysical Society Forty-Third Annual Meeting, Baltimore, MD, Feb 13-17, 1999.

* To whom correspondence should be addressed. Telephone: 55-11-818-2155. Fax: 55-11-815-5579. E-mail: fdcreina@iq.usp.br.

[1] Abbreviation: RLC, myosin regulatory light chain.

10.1021/bi9924718 CCC: $19.00
Published on Web 03/11/2000

The amino acid sequence in site I of RLC is (*11*):

							1		3		5		7		9			12					
F	K	E	A	F	N	M	I	**D**	Q	**N**	R	**D**	G	**F**	I	**D**	K	E	**D**	L	H	D	M	L	A	S	M
α-helix								loop												α-helix							

We have previously demonstrated that replacing the aspartate in the 9th position with a glutamate (D9E) reduced the site affinity, while the same substitution in position 12 (D12E) increased the site affinity and changed the specificity, converting the Ca^{2+}/Mg^{2+} site into a Ca^{2+}-specific site (*5*).

A possible reason for the reduced affinity of mutant D9E is that this mutation could affect the interactions that occur between positions 5 and 9, making the site unstable. In most EF-hand structures already determined, position 9 interacts with the side chain in position 5 by hydrogen bonding. In some proteins that have a glutamate at position 9, it makes a hydrogen bond with a serine in position 5; in those proteins where the ion is coordinated by a water molecule in position 9, it makes a hydrogen bond with the residue in position 5, usually aspartate or asparagine. A glutamate in position 9 cannot make a hydrogen bond with an aspartate in position 5, as in the mutant D9E (*13*, *14*).

Even though in some EF-hand sites the side chain of position 12 seems not to participate in Mg^{2+} binding (*15*), this is probably not the case in gizzard RLC. Scallop RLC has a high degree of homology with gizzard RLC (*16*), and its crystal structure shows that the aspartate in position 12 coordinates Mg^{2+} binding with only one oxygen from the side chain (*17*). Observations with mutant D12E support the idea that site specificity depends on the side chain of the amino acid in position 12, coordinating Mg^{2+} with one oxygen (octahedral coordination) and Ca^{2+} with two oxygens (pentagonal bipyramidal coordination). In the wild-type RLC, the aspartate in position 12 may rotate and accommodate either Mg^{2+} or Ca^{2+}. When the longer side chain of glutamate is present in the mutant RLC site, its rotation would be sterically blocked into the bidentate configuration, making the site Ca^{2+}-specific (*5*).

To further investigate these mechanisms of affinity and specificity and to gain insight into how the residues in the site interact, double mutant cycles were used (*18*). Three positions were chosen: 9 and 12, where the substitution of the aspartate by a glutamate had already produced changes in site affinity and specificity (D9E and D12E) (*5*), and position 5, where the aspartate was replaced by a serine (D5S). Serine in position 5 mimics the CD site of parvalbumin, where a serine in this position interacts with a glutamate in position 9. All the possible combinations were studied: the single mutants D5S, D9E, and D12E; the double mutants D5S/D9E, D5S/D12E, and D9E/D12E; and the triple mutant D5S/D9E/D12E. The seven mutants plus the wild-type RLC complete six double mutant cycles.

With the use of double mutant sites, it is possible to analyze intra-site cooperativity, evaluate pairwise interactions between positions, and measure to what extent each position interferes with the others' interactions with ions (*18*). If the effects of a mutation at a particular position suffer any change in the presence or absence of a mutation in another position, it suggests that the interaction of the first position with the ion was affected by a mutation in the second location. Hence, the two positions have some kind of interaction (*19*). This interaction can be direct (hydrogen bonding between coordinating side chains, for instance), conformational (the second mutation affects the loop backbone conformation), or through the bound ion. A typical double mutant cycle is shown below:

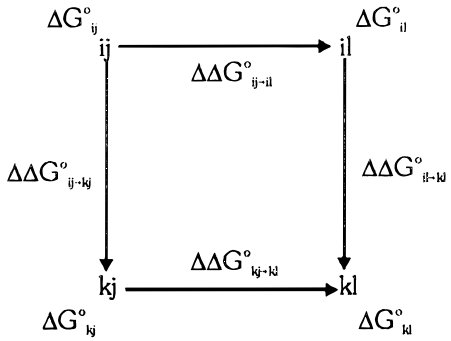

The cycle includes wild-type protein (ij), two simple mutants (il and kj), and the corresponding double mutant (kl). From ion dissociation constants, it is possible to calculate the apparent free energy of ion binding (ΔG_{ij}) and the effects of each mutation on this energy ($\Delta\Delta G_{ij\rightarrow il}$**)**. The energy difference between the double mutant and the two single mutants taken separately can be defined as the coupling energy, and calculated from the equation (*20*):

$$\Delta\Delta G^{\circ}_{i\leftrightarrow j} = \Delta\Delta G^{\circ}_{il\rightarrow kl} - \Delta\Delta G^{\circ}_{ij\rightarrow kj} = \Delta\Delta G^{\circ}_{kj\rightarrow kl} - \Delta\Delta G^{\circ}_{ij\rightarrow il} \quad (1)$$

where i and j are the amino acids in wild-type protein and k and l are the mutations.

If the effect of the double mutation is not equal to the sum of effects of the two single mutations, the interaction between them can be measured by the coupling energy (*20*). A negative value of the coupling energy indicates a favorable interaction; that is, the double mutant is less destabilizing (or more stabilizing) than expected from the sum of the single mutants (*21*).

When a pair of mutations have a coupling energy with the same value as all other pairs of mutations, the most probable explanation is that the mutations involved have some nonspecific effect over all the other positions, for instance, causing a conformational change that affects the whole site, or transmitting the changes through the ion. When there is a coupling energy unique to only two positions, it probably reflects a more specific interaction, such as hydrogen bonding, directly or through a water molecule (*19*).

The D12E mutation increases RLC Ca^{2+} affinity and specificity (*5*). In the present work, we observe that this effect is independent of the other positions, and occurs in all the studied mutants. This is not a general rule, as many Ca^{2+}/Mg^{2+} sites have glutamate in position 12 (*5*). We concluded that positions 5 and 9 in RLC can interact in different ways in the binding of Ca^{2+} or Mg^{2+} and probably have a direct interaction when Mg^{2+} is bound to the mutant D5S/D9E, since the coupling energy is large and negative. If these two positions have a direct interaction, the glutamate in position 9 can coordinate directly the Mg^{2+} ion, as in parvalbumin site I. Our results suggest that this interaction does not occur when a glutamate is in position 12 (in D5S/D9E/D12E) or with Ca^{2+}, because in these situations the coupling energies are smaller. Since the RLC site is more closed than other

EF-hand sites, this site is probably too small for a direct coordination in position 9, either with a longer side chain in position 12 or with a larger ion.

MATERIALS AND METHODS

Chemical Reagents. All reagents were analytical grade. Milli-Q deionized water (Millipore Corp.) was used in all experiments. Dialysis tubing used in flow dialysis was Spectra/Por #2 (with molecular mass cutoff of 12−14 kDa), manufactured by Spectrum Medical Industries.

Construction, Expression, and Purification of Mutant RLCs. Mutant RLCs D9E and D12E were previously produced (*5*). A cDNA encoding chicken smooth muscle myosin regulatory light chain (*11*), cloned in M13mp19 (*5*), was used for mutagenesis. All mutations were performed as described (*22*), using the following oligonucleotides: D5S, 5′CCAGAACCGTTCCGGGTTCATT; D12E, 5′AGAAGGAGGAGCTGCATGACA.

Double mutants were produced by performing the second mutation on the mutant template. For D5S/D9E and D5S/D12E, mutation D5S was performed on D9E and D12E templates, respectively. For D9E/D12E and the triple mutant D5S/D9E/D2E, mutation D12E was performed on D9E and D5S/D9E double mutant templates. The whole RLC cDNA was sequenced and used to replace the wild-type cDNA fragment between the *Hin*dIII/*Eco*RI sites in RLC-pMW172 (*23*). The correct insertion of only one copy of the fragment was checked by digestion with *Nco*I/*Pst*I. Recombinant RLC was expressed and purified as described (*5*).

Direct Ca^{2+} Binding Measurements. Ca^{2+} was removed from recombinant RLCs as described (*24*). Ca^{2+} binding was measured by flow dialysis, as described (*24*), with some modifications. The procedures were the same as previously described (*5*), except for protein concentrations and the dialysis tubing. In this work, we used Spectra/Por dialysis tubing, while in a previous work (*5*) Servapor dialysis tubing was used. Protein concentration in the assay was between 43 and 70 μM (molecular mass of recombinant RLC is 19.8 kDa). The assay solution contained 50 mM NaCl, 20 mM imidazole, pH 7.0, and 2 mM 2-mercaptoethanol. Ca^{2+} contamination in the buffers was below 10^{-6} M, as previously determined by atomic absorption spectroscopy (*5*). The concentrations of $CaCl_2$ stocks were 5 and 40 mM, as determined by titration with $Hg(NO_3)_2$. Aliquots of 5−25 μL of the $CaCl_2$ solutions were added every fifth fraction. The final addition of $CaCl_2$ (50 μL of 1 M stock) was added at fraction 55. At least three data sets of each mutant or wild-type RLC were fitted independently to eq 2, using an iterative nonlinear regression curve-fitting procedure:

$$y = \frac{n_1'[Ca^{2+}]}{[Ca^{2+}] + K_{Ca^{2+}}} \quad (2)$$

where y is the measured portion of sites filled at each $[Ca^{2+}]$, $K_{Ca^{2+}}$ is the apparent dissociation constant, and n_1' is a correction factor for nonspecific binding. Values greater than 1 indicate nonspecific binding to the surface of dialysis membrane and chamber walls, while smaller values suggest that a fraction of the protein is inactive.

Mg^{2+} apparent dissociation constants were calculated from the ability of Mg^{2+} to displace bound Ca^{2+}. The protein was used in competition assays at the same concentrations used in Ca^{2+} binding assays, in the same buffer, in the presence of 40 μM $CaCl_2$. Aliquots of 2−40 μL of 250 mM $MgCl_2$ were added every fifth fraction. The final addition was of $CaCl_2$, to a final concentration of 10 mM. At least three data sets were fitted to eq 3, using an iterative nonlinear regression curve-fitting procedure:

$$y' = \frac{[Ca^{2+}]K_{Mg^{2+}}}{n_2'(K_{Mg^{2+}}K_{Ca^{2+}} + K_{Ca^{2+}}[Mg^{2+}] + K_{Mg^{2+}}[Ca^{2+}])} \quad (3)$$

where y' is the measured portion of sites filled with Ca^{2+} at each $[Mg^{2+}]$, $K_{Ca^{2+}}$ and $K_{Mg^{2+}}$ are the apparent dissociation constants for Ca^{2+} and Mg^{2+}, respectively, and n_2' is a correction factor for nonspecific binding. $K_{Ca^{2+}}$ was obtained from eq 2.

Calculation of Free Energies. The changes in the apparent binding free energy (*18*) due to each mutation were calculated from the apparent dissociation constants (for each ion), according to eq 4:

$$\Delta\Delta G^\circ_{app} = -RT \ln(K_i/K_f) \quad (4)$$

where K_i and K_f are the dissociation constants before and after each mutation. Here, mutations that increase Ca^{2+} or Mg^{2+} affinities have negative $\Delta\Delta G^\circ_{app}$. Using double mutant cycles (*19*), the coupling energy between each pair of mutations was calculated, in the presence or absence of the third mutation, and with Ca^{2+} and Mg^{2+}, from eq 1.

Error propagation was calculated according to eq 5:

$$s_{\bar{w}}^2 = \left(\frac{\partial w}{\partial x}\right)_{\bar{w}}^2 s_{\bar{x}}^2 + \left(\frac{\partial w}{\partial y}\right)_{\bar{w}}^2 s_{\bar{y}}^2 \quad (5)$$

where s is the standard deviation, w is the resulting function, and x and y are the initial functions (*25*, *26*).

RESULTS

Ca^{2+} and Mg^{2+} Affinities. To study the determinants of metal affinity and specificity in the RLC, five mutants were produced and compared with wild-type protein and two previously produced mutants (*5*). All mutants contain from one to three point mutations in coordinating positions along the EF-hand site. Wild-type and mutant proteins were expressed, purified, and analyzed by flow dialysis, to determine Ca^{2+} and Mg^{2+} affinities.

The effects of the mutations on Ca^{2+} affinity are presented in Figure 1A and Table 1. Single mutations D5S and D9E reduce Ca^{2+} affinity. The double mutant D5S/D9E has this effect intensified. All RLCs containing the mutation D12E have affinities for Ca^{2+} greater than wild type. The single mutant D12E has the highest Ca^{2+} affinity, while the double mutant D9E/D12E has higher affinity than wild type, and D5S/D12E has a Ca^{2+} affinity similar to wild type. The triple mutant D5S/D9E/D12E has higher affinity than wild type, but lower than D9E/D12E.

The sites in low-affinity mutants (D5S, D9E, and D5S/D9E) did not saturate in the assays. The dissociation constants were calculated from the partial binding curves obtained, using eq 2. Since n_1' tends to be overestimated when the site does not saturate during the assay, the maximum value accepted for n_1' in the fitting was 1. To

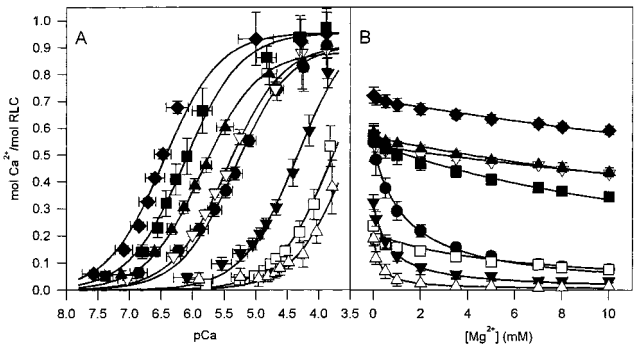

FIGURE 1: Ca^{2+} binding to recombinant smooth muscle RLC (●) and mutants: D5S (□), D9E (▼), D12E (◆), D5S/D9E (△), D5S/D12E (▽), D9E/D12E (■), and D5S/D9E/D12E (▲). (A) The binding of $^{45}Ca^{2+}$ was measured as a function of free Ca^{2+} concentration. (B) The ability of Mg^{2+} to displace bound $^{45}Ca^{2+}$ was measured as a function of Mg^{2+} concentration. Each data point represents the mean of at least three independent assays. Standard deviations are shown as bars. The curves were calculated from the mean dissociation constants shown in Table 1, according to eqs 2 and 3.

ascertain the validity of this restriction, nonspecific binding was determined in the absence of protein and shown to contribute to less than 3% of the binding. No measurement points at $[Ca^{2+}]$ higher than 1 mM were added to the assay, because at these higher $[Ca^{2+}]$ the assay is not reliable due to nonspecific binding of calcium to charged surfaces at these high calcium concentrations.

The results of Mg^{2+} competition assays are summarized in Figure 1B and Table 1. All mutants bind Mg^{2+} with lower affinities than wild-type RLC. However, the decrease in affinity varies from 1.5 (D5S/D9E) to 33 times (D5S) the wild-type values. The greatest changes occurred when mutation D5S was present, either alone or in the double mutant D5S/D12E. The mutations in positions 9 or 12 had small effects on Mg^{2+} affinity on their own, while mutation D9E greatly reduces the effects of D5S.

Site specificities can be measured by the ratio $K_{Mg^{2+}}/K_{Ca^{2+}}$. The low-affinity mutants—D5S, D9E, and D5S/D9E—also have low specificity. D5S/D9E has almost no specificity, and binds Ca^{2+} and Mg^{2+} with similar affinities. D12E-containing mutants have higher Ca^{2+} specificity than wild type. The single mutant D12E has the highest specificity, 37 times that of wild-type protein. Specificity decreases from D12E to D5S/D12E, then to the triple mutant, and finally to the double mutant D9E/D12E, which is 12 times more Ca^{2+}-specific than wild type. Greater Ca^{2+} specificity can result mainly from greater Ca^{2+} affinity (D12E and D9E/D12E) or from lower Mg^{2+} affinity (D5S/D12E and D5S/D9E/D12E); lower Ca^{2+} specificity usually results mainly from lower Ca^{2+} affinities.

Higher Ca^{2+} affinity and specificity for D12E and lower Ca^{2+} affinity and specificity for D9E have been described previously (*5*) and are confirmed in this work. It was reported that D9E showed a 2-fold reduction in Ca^{2+} affinity, while D12E showed a 2-fold increase in Ca^{2+} affinity. In the present work, D9E shows a 10-fold reduction, and D12E shows a 10-fold increase. Besides that, protein saturation occurs with less ligand bound per mole of protein [lower nonspecific binding; see n_1' values in Table 1 and in (*5*)]. The larger measured effects of both mutations are probably a consequence of this lower nonspecific binding. These changes also affect the Mg^{2+} dissociation constants. These differences in nonspecific binding result from some changes in methodology, especially in the type of the dialysis tubing used (as described under Materials and Methods).

Binding and Coupling Energies. From the dissociation constants in Table 1, the changes in the apparent binding energy were calculated, and the six double mutant cycles are represented as a cube for each ion used in Figure 2. All mutations cause changes in the binding energy in at least three of the possible site environments. In the presence of Ca^{2+} (Figure 2A), mutation D5S (horizontal arrows) always causes positive changes in binding energies, D9E (vertical arrows) can cause both negative and positive changes, and D12E (diagonal arrows) always causes negative changes. These results show that mutation D5S always lowers Ca^{2+} affinity and D12E always increases Ca^{2+} affinity, no matter what amino acids are in the other positions. D9E, however, can have different effects depending on the other positions in the site. In the presence of Mg^{2+} (Figure 2B), D9E and D12E can cause positive or negative changes depending on the amino acids in the other positions of the site, while D5S can cause positive changes or have no significant effect.

Coupling energies are a measure of how much two positions affect each other in a protein, either directly or through conformational changes, and any value different from zero indicates some interaction. Negative values indicate favorable interactions, stabilizing the ion binding, while positive values indicate destabilizing interactions. The coupling energies between each pair of mutations were calculated for Ca^{2+} and Mg^{2+} binding, according to eq 5, in the presence and absence of the third mutation (Table 2). For Ca^{2+} binding, all the coupling energies are negative, about 1 kcal/mol or a little lower. For Mg^{2+} binding, the coupling energy between D5S and D9E is larger than the others (−2.33 kcal/mol) in the presence of an aspartate in position 12, and smaller than the others (−0.5 kcal/mol) when a glutamate is present in the 12th position. Mutation D12E decreases almost 5 times the interaction between positions 5 and 9. The coupling energies between D5S and D12E and between D9E and D12E are negative in the absence of the third mutation, but become positive when the third mutation is present.

The coupling energy results suggest that an interaction between the serine in position 5 and the glutamate in position 9 is formed when the double mutant D5S/D9E binds magnesium. The smaller values for Ca^{2+} binding and in the presence of mutation D12E suggest that the interaction does not occur in these situations.

DISCUSSION

Ca^{2+} and Mg^{2+} Affinities. Mutation D5S has the greatest negative effects on both Ca^{2+} and Mg^{2+} binding. Two possible reasons for that are (i) the loss of a negative charge when serine replaces aspartate and (ii) the effects on the coordinating water in position 9. When an aspartate or an asparagine is in position 5, the side chain may make a hydrogen bond with a water molecule in position 9 (*13*). This hydrogen bond stabilizes the water in a coordinating position, and cannot be performed by a serine. Therefore, the lower affinity in the D5S mutant may be a consequence of modifications in two coordinating positions: 5 (loss of a charge) and 9 (weaker interactions with the water molecule).

Table 1: Dissociation Constants

RLC	$K_{Ca^{2+}}$ (n_1')[a] (μM)	$K_{Mg^{2+}}$ (n_2')[a] (μM)	$K_{Mg^{2+}}/K_{Ca^{2+}}$
wild type	4.7 ± 1.0 (0.9 ± 0.1)	139 ± 15 (1.7 ± 0.2)	29 ± 7
D5S	166 ± 42 (1)[b]	4629 ± 749 (0.95 ± 0.08)	28 ± 8
D9E	46 ± 9 (1)[b]	376 ± 79 (1.5 ± 0.1)	8 ± 2
D12E	0.34 ± 0.12 (0.96 ± 0.09)	370 ± 52 (1.34 ± 0.05)	1078 ± 405
D5S/D9E	308 ± 108 (1)[b]	250 ± 184 (0.65 ± 0.07)	0.8 ± 0.7
D5S/D12E	3.5 ± 0.3 (0.91 ± 0.03)	3145 ± 491 (1.65 ± 0.02)	885 ± 155
D9E/D12E	0.75 ± 0.13 (0.95 ± 0.06)	268 ± 22 (1.7 ± 0.1)	359 ± 70
D5S/D9E/D12E	1.4 ± 0.3 (0.88 ± 0.08)	988 ± 68 (1.64 ± 0.04)	700 ± 135

[a] Apparent Ca^{2+} and Mg^{2+} dissociation constants ($K_{Ca^{2+}}$ and $K_{Mg^{2+}}$) and correction factors for nonspecific binding (n_1' and n_2') are presented as mean ± SD. Ca^{2+} dissociation constants were obtained by fitting each set of data from Ca^{2+} bound/RLC versus [Ca^{2+}] to eq 1, and averaging the resulting constants ($n \geq 3$). Mg^{2+} constants were obtained by fitting each set of data from Ca^{2+} bound/RLC versus [Mg^{2+}] to eq 2, and then averaging ($n \geq 3$). $K_{Ca^{2+}}$ was obtained from eq 1. [b] n_1' was set to 1 because it tends to be overestimated when the site does not saturate during the assay.

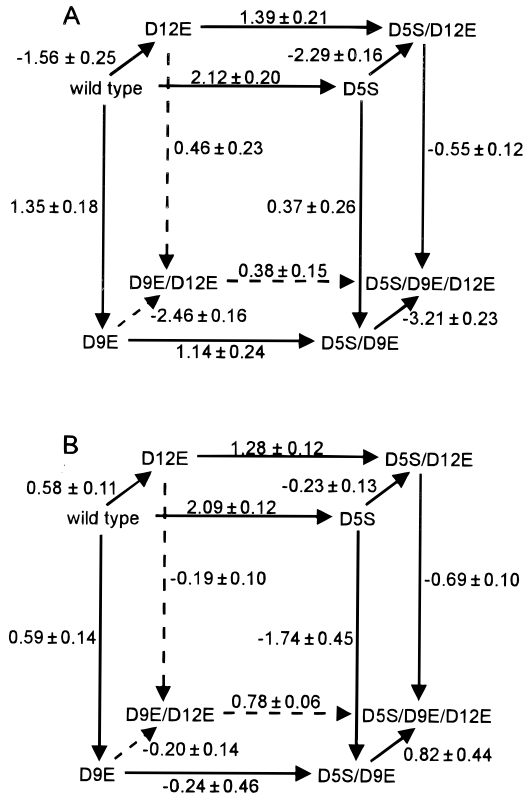

FIGURE 2: Changes in apparent binding free energy ($\Delta\Delta G^{\circ}_{app}$) caused by each mutation, in kcal/mol, calculated according to eq 4. (A) Calculated from Ca^{2+} apparent dissociation constants. (B) Calculated from apparent Mg^{2+} dissociation constants.

Table 2: Coupling Energies between the Involved Mutations

coupled mutations	$\Delta\Delta G^{\circ}_{Ca^{2+}}$[a]	$\Delta\Delta G^{\circ}_{Mg^{2+}}$[a]	background[b]
D5S ↔ D9E	−0.99 ± 0.31	−2.33 ± 0.47	wild type
	−1.01 ± 0.26	−0.50 ± 0.14	D12E
D5S ↔ D12E	−0.73 ± 0.29	−0.81 ± 0.17	wild type
	−0.76 ± 0.28	+1.02 ± 0.46	D9E
D9E ↔ D12E	−0.89 ± 0.29	−0.79 ± 0.17	wild type
	−0.92 ± 0.28	+1.05 ± 0.46	D5S

[a] In kcal/mol. The energies were calculated from mean Ca^{2+} and Mg^{2+} dissociation constants, and the error was propagated. [b] Amino acids present at positions not involved in the mutations.

The substitution of an aspartate in position 5 by a serine also resulted in lower Ca^{2+} affinity in the EF site of oncomodulin, while the inverse mutation (serine to aspartate) in the CD site of oncomodulin resulted in higher Ca^{2+} affinity (*27*). The same effects were observed comparing synthetic peptides containing serine or aspartate in position 5 (*28*). Serine in position 5 seems to lower Ca^{2+} affinity, no matter what amino acids are in the other positions.

The single mutant D9E also lowers Ca^{2+} and Mg^{2+} affinities, as previously described (*5*). Since glutamate has a longer side chain than the original aspartate, the lower affinities can result from a steric effect, stronger for Ca^{2+} (a bigger ion) than for Mg^{2+}, as seen from the dissociation constants (10 times reduction for Ca^{2+}, 2.7 times reduction for Mg^{2+}). The effect of side chain length at position 9, however, depends on residues at other positions within the site: in the context of the double mutant D5S/D12E, the D9E mutation actually increases both Ca^{2+} and Mg^{2+} affinities approximately 3-fold (compare D5S/D12E with D5S/D9E/D12E in Table 1).

Aspartate in the 9th position was reported to result in greater Ca^{2+} affinity than glutamate in position 9, in different situations (*28*−*30*). However, in the CD site of oncomodulin, this replacement leads to a higher Ca^{2+} affinity (*6*), reinforcing the notion that Ca^{2+} affinity is determined by multiple factors and interactions.

The effect of mutation D12E has been described as locking the side chain of the 12th position in the bidentate conformation, therefore favoring Ca^{2+} binding (*5*). A glutamate in position 12 is able to revert the negative effects of mutations D5S and D9E in Ca^{2+} affinity and to make the site more Ca^{2+}-specific, independent of the amino acids at positions 5 and 9. However, many naturally occurring proteins bind Mg^{2+} as well as Ca^{2+} with a glutamate at position 12 (*31*), indicating that the key for D12E mutant specificity is the conformation of other amino acids which create a metal binding cavity not capable of accommodating the longer side chain of a glutamate in a Mg^{2+} binding conformation. Since mutations inside the site did not much affect the specificity of the D12E mutants (compare D12E, D5S/D12E, D9E/D12E, and D5S/D9E/D12E in Table 1), the cavity size might be the result of a more closed loop, stabilized by long-range interactions. Figure 3A shows that RLC has a more closed loop than troponin C site III, a Ca^{2+}/Mg^{2+} site with high homology to the single mutant D12E. In troponin C, the glutamate side chain in position 12 occupies the same position as the aspartate side chain in RLC, and both side chains are probably able to rotate. The longer side chain of a glutamate in D12E is probably too big to rotate into a Mg^{2+} binding conformation in a more closed site, and it binds Ca^{2+} with much higher affinity than Mg^{2+}.

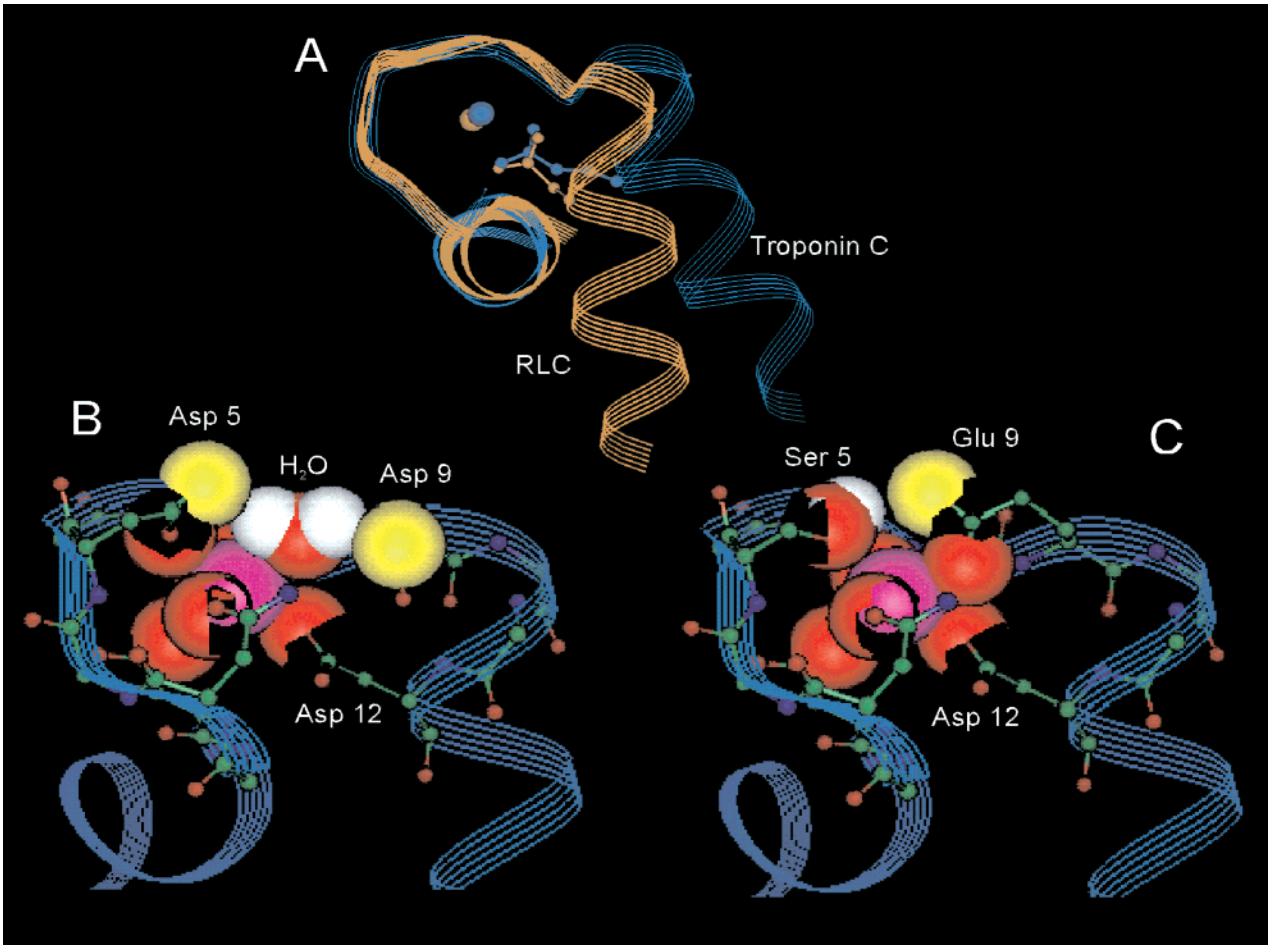

FIGURE 3: (A) Ion binding loop structures from scallop RLC (*17*) (orange) and troponin C site III (*35*) (blue), showing that the RLC loop is more closed than troponin C, a probable reason for greater Ca^{2+} specificity of D12E. (B and C) Models for Mg^{2+} coordination in smooth muscle RLC EF-hand site: (B) wild type; (C) D5S/D9E. The Mg^{2+} ion (pink) is coordinated by six oxygens (red). One of the coordinating oxygens is behind the ion. Hydrogens are shown in white, and oxygens participating in hydrogen bonds are colored yellow. In the wild-type protein (B), a water oxygen coordinates the ion, and the water hydrogens make hydrogen bonds with side chain oxygens from positions 5 and 9. In D5S/D9E (C), the glutamate in position 9 can coordinate the Mg^{2+} ion directly, and make a hydrogen bond with the serine in position 5. Mg^{2+} coordination in (B) is much tighter than in (A). It is easy to imagine that a longer side chain—like a glutamate in position 12 (mutation D12E)—or a bigger Ca^{2+} ion would not fit in this site configuration. (A) was constructed with the coordinates from troponin C site III (*35*) (5TNC, Protein Data Bank) and scallop RLC site I (*17*) (1WDC, Protein Data Bank), while (B) and (C) were modeled from scallop RLC site I (*17*) (1WDC, Protein Data Bank) using the software Insight II (Molecular Simulations Inc.) on a Silicon Graphics Indigo^2.

Although many natural sites associate relatively low Ca^{2+} affinity with high Ca^{2+} specificity, and high Ca^{2+} affinity to Mg^{2+} binding (*32*), this correlation cannot be assumed to be a general rule. Wild-type RLC has a low ($\sim 10^{-6}$ M) Ca^{2+} affinity and binds Mg^{2+} ($K_{Mg^{2+}} \sim 10^{-4}$ M), while the mutant D5S/D12E has about the same Ca^{2+} affinity and is Ca^{2+}-specific ($K_{Mg^{2+}} > 10^{-3}$ M).

Binding and Coupling Energies. We observed that the change in binding free energy caused by each mutation depends greatly on which amino acid is present at the other positions, indicating that the three studied positions interact with each other, as expected for amino acids so closely located in protein structure.

Coupling energy calculations yield different results when Ca^{2+} or Mg^{2+} dissociation constants are used (see Table 2). When calculated from Ca^{2+} constants, all the coupling energies have approximately the same value, indicating a similar level of interaction among all the studied residues in the presence of Ca^{2+}. Since pairs of residues in the three positions have the same coupling energy values and are independent of the third position (even when this position interacts with the other two), these interactions are probably nonspecific, and arise from structural changes in the site (*33*), propagated either through the protein backbone or through the ion binding site.

When calculated from Mg^{2+} constants, however, the coupling energies have different values. The coupling energies between D12E and any other mutation (D5S or D9E) are negative in the absence of the third mutation, and positive when the third mutant is present. On the other hand, D5S and D9E can be highly coupled when an aspartate is at position 12, or poorly coupled when a glutamate is substituted in position 12, but the coupling energy between these positions is always negative.

A negative coupling energy means that the double mutant is less destabilizing than the sum of the single mutants, indicating that both single mutations disrupt the same interaction, with nonadditive effects, or even that a new favorable interaction is formed in the double mutant. A positive coupling energy suggests that the double mutant disrupts some interaction that is not affected or even created by a single mutation.

The difference in coupling energies in the presence of Ca^{2+} or Mg^{2+} indicates that at some point in the double mutant cycle the binding of Mg^{2+} and Ca^{2+} are significantly different. Since the largest negative coupling energy is between D5S and D9E, in the presence of Mg^{2+} (with aspartate in position 12), it suggests that an interaction between positions 5 and 9 occurs when Mg^{2+} is bound, and that this interaction is not present when Ca^{2+} is bound.

The double mutant D5S/D9E has greater affinity for Mg^{2+} than the single mutants D5S and D9E, suggesting that a stabilizing interaction is formed in the double mutant, compensating for the original interactions that were disrupted by the single mutations. Figure 3B,C presents models of the interactions in the wild-type protein and in D5S/D9E. The interaction between the aspartates in the 5th and 9th positions usually occurs through the water molecule that coordinates the ion, and this is the interaction expected for wild-type RLC (Figure 3B). When serine and glutamate are in these positions, however, they can interact directly through a hydrogen bond between their side chains, as in parvalbumin site I. In these sites, the glutamate in position 9 coordinates the ion directly (*13*). This interaction is possible in the mutant D5S/D9E (Figure 3C). Therefore, in this mutant, the glutamate in position 9 may be able to coordinate Mg^{2+} directly. For steric reasons, it would not be possible to directly coordinate Ca^{2+}, a larger ion, or to coordinate Mg^{2+} directly when a glutamate is in position 12, as in D5S/D9E/D12E. The positive values for the coupling energies between D12E and any other mutation (D5S or D9E), when the third mutant is present, are consequences of this interaction: in these cycles, a single mutation stabilizes the site, forming an interaction that is disrupted or weakened in the double mutant. The coupling energy is therefore positive, indicating that the double mutant is more destabilizing than expected from the sum of the single mutants.

Besides comparing pairs of mutants in each double mutant cycle, pairs of cycles can be compared in the cubes from Figure 2. The difference between coupling energies from two opposite sides in the cube is a measure of how much one mutation affects the interaction between the other two (*19*). When all interactions in a site are nonspecific, one mutation does not affect the interaction between the other two. When there is a specific interaction, which can be disrupted if any structural changes are caused by a mutation in another position, this value will be different from zero.

In the presence of Ca^{2+}, this difference of coupling energies is zero, indicating that each cycle is independent from the other mutation. In the presence of Mg^{2+}, the difference between the coupling energies in any two opposite sides of the cube is -1.84 ± 0.49 kcal/mol, showing that one mutation affects the interaction between the other two positions. This observation further supports the idea that these positions in the RLC EF-hand site interact in a more specific way when Mg^{2+} is bound than when the site is occupied by Ca^{2+}.

Natural Homologues. When the primary sequences of wild-type and mutant RLCs are compared with 273 naturally occurring EF-hand proteins (*16*) (Table 3), the low-affinity mutants (D5S, D9E, and D5S/D9E) have no homologues in the mutated positions. Maybe these combinations are intrinsically unstable, and do not depend on the other positions of the site. *Drosophila* nonmuscle RLC has 11 out of 12 site positions equal to the mutant D9E, but its affinity for divalent cations is not known.

Table 3: RLC Mutants and Their Natural Homologue Sites

mutant	amino acid in position 5	9	12	natural homologue[a]
wild type	D	D	D	RLC
D5S	S	D	D	not found
D9E	D	E	D	*Drosophila* nonmuscle RLC
D12E	D	D	E	troponin C site III
D5S/D9E	S	E	D	not found
D5S/D12E	S	D	E	troponin C site II
D9E/D12E	D	E	E	calbindin 28 kDa site IV
D5S/D9E/D12E	S	E	E	parvalbumin site I

[a] Site sequences are the consensus of sequences reviewed by Kawasaki and Kretsinger (*16*).

The double mutant D5S/D12E has the same amino acids in the three studied positions as troponin C site II, a Ca^{2+}-specific site, while the triple mutant, D5S/D9E/D12E, has the same amino acids as parvalbumin site I, which is considered a Ca^{2+}/Mg^{2+} site, although the affinity ratio is larger than 3 orders of magnitude (*34*). In both cases, the only coordinating amino acid with a different side chain is in position 3, occupied by an asparagine in RLCs and by an aspartate in the other examples.

The double mutant D9E/D12E has the same amino acids as calbindin 28 kDa site IV in all coordinating positions, and D12E has the same amino acids as chicken troponin C site III in 9 out of 12 site positions. The three different amino acids are in nonconserved positions. However, troponin C site III (Figure 3) is not Ca^{2+}-specific, while the mutant is.

The coupling energy results lead to the conclusion that in RLC EF-hand site positions 5 and 9 can interact in different ways depending on the bound ion. When the site binds Mg^{2+}, this interaction is probably similar to the one found in parvalbumin site I. In this case, the glutamate in position 9 coordinates the ion directly. This interaction does not occur when a glutamate is in position 12 (in D5S/D9E/D12E) or when Ca^{2+} is bound, probably due to steric constraints in a more closed loop conformation. Since some Ca^{2+}/Mg^{2+} sites have the same coordinating positions as some Ca^{2+}-specific mutants, we confirmed that the key for specificity is in the site tertiary structure, not in any particular position.

ACKNOWLEDGMENT

We thank Drs. Chuck S. Farah and Ana C. R. da Silva for critical reading of the manuscript.

REFERENCES

1. McPhalen, C. A., Strynadka, N. C. J., and James, M. N. G. (1991) *Adv. Protein Chem. 42*, 77−144.
2. Heaton, F. W. (1993) in *Magnesium and the cell* (Birch, N. J., Ed.) pp 121−136, Academic Press Ltd., London.
3. Falke, J. J., Drake, S. K., Hazard, A. L., and Peersen, O. B. (1994) *Q. Rev. Biophys. 27*, 219−290.
4. Kretsinger, R. H. (1987) *Cold Spring Harbor Symp. Quant. Biol. 52*, 499−510.
5. Da Silva, A. C. R., Kendrick-Jones, J., and Reinach, F. C. (1995) *J. Biol. Chem. 270*, 6773−6778.
6. Hapak, R. C., Lammers, P. J., Palmisano, W. A., Birnbaum, E. R., and Henzl, M. T. (1989) *J. Biol. Chem. 264*, 18751−18760.
7. Linse, S., and Forsén, S. (1995) *Adv. Second Messenger Phosphoprotein Res. 30*, 89−151.

8. Kretsinger, R. H., and Nockolds, C. E. (1973) *J. Biol. Chem. 248*, 3313−3326.
9. Moncrief, N. D., Kretsinger, R. H., and Goodman, M. (1990) *J. Mol. Evol. 30*, 522−562.
10. Bagshaw, C. R., and Kendrick-Jones, J. (1980) *J. Mol. Biol. 140*, 411−433.
11. Messer, N. G., and Kendrick-Jones, J. (1988) *FEBS Lett. 234*, 49−52.
12. Bagshaw, C. R., and Kendrick-Jones, J. (1979) *J. Mol. Biol. 130*, 317−336.
13. Strynadka, N. C. J., and James, M. N. G. (1989) *Annu. Rev. Biochem. 58*, 951−998.
14. Herzberg, O., and James, M. N. G. (1985) *Biochemistry 24*, 5298−5302.
15. Malmendal, A., Evenäs, J., Thulin, E., Gippert, G. P., Drakenberg, T., and Forsén, S. (1998) *J. Biol. Chem. 273*, 28994−29001.
16. Kawasaki, H., and Kretsinger, R. H. (1994) *Protein Profiles 1*, 343−517.
17. Houdusse, A., and Cohen, C. (1996) *Structure 4*, 21−32.
18. Carter, P. J., Winter, G., Wilkinson, A. J., and Fersht, A. R. (1984) *Cell 38*, 835−840.
19. Horovitz, A., and Fersht, A. R. (1990) *J. Mol. Biol. 214*, 613−617.
20. Faiman, G. A., and Horovitz, A. (1996) *Protein Eng. 9*, 315−316.
21. Frisch, C., Schreiber, G., Johnson, C. M., and Fersht, A. R. (1997) *J. Mol. Biol. 267*, 696−706.
22. Carter, P., Bedouelle, H., and Winter, G. (1985) *Nucleic Acids Res. 13*, 4431−4443.
23. Rowe, T., and Kendrick-Jones, J. (1992) *EMBO J. 11*, 4715−4722.
24. Da Silva, A. C. R., De Araujo, A. H. B., Herzberg, O., Moult, J., Sorenson, M., and Reinach, F. C. (1993) *Eur. J. Biochem. 213*, 599−604.
25. Helene, O. A. M., and Vanin, V. R. (1981) in *Tratamento estatístico de dados em Física experimental*, Editora Edgard Blucher Ltda., São Paulo, Brazil.
26. Taylor, J. K. (1990) in *Statistical techniques for data analysis*, Lewis Publishers, Boca Raton, FL.
27. Henzl, M. T., Hapak, R. C., and Likos, J. J. (1998) *Biochemistry 37*, 9101−9111.
28. Reid, R. E., and Procyshyn, R. M. (1995) *Arch. Biochem. Biophys. 323*, 115−119.
29. Drake, S. K., Lee, K. L., and Falke, J. J. (1996) *Biochemistry 35*, 6697−6705.
30. Procyshyn, R. M., and Reid, R. E. (1994) *Arch. Biochem. Biophys. 311*, 425−429.
31. Marsden, B. J., Shaw, G. S., and Sykes, B. D. (1990) *Biochem. Cell Biol. 68*, 587−686.
32. Reid, R. E., and Hodges, R. S. (1980) *J. Theor. Biol. 84*, 401−444.
33. Hidalgo, P., and MacKinnon, R. (1995) *Science 268*, 307−310.
34. Tanokura, M., Imaizumi, M., and Yamada, K. (1986) *FEBS Lett. 209*, 77−82.
35. Herzberg, O., and James, M. N. G. (1988) *J. Mol. Biol. 203*, 761−779.

BI9924718